



Original Article



## Protective effect of exosomes derived from bone marrow mesenchymal stem cells on hypoxia reperfusion injury of cardiomyocytes

Di Zhao<sup>1</sup>, Yanling Bu<sup>2</sup>, Haifeng Shao<sup>1</sup>, Jian Wang<sup>1</sup>, Wenhua Li<sup>1</sup>, Qiang Li<sup>1\*</sup>

<sup>1</sup> Department of Cardiology I, The Third Affiliated Hospital of Qiqihar Medical University, Qiqihar 161000, China

<sup>2</sup> Department of Ultrasound, The Third Affiliated Hospital of Qiqihar Medical University, Qiqihar 161000, China

### Article Info

### Abstract



#### Article history:

**Received:** October 24, 2023

**Accepted:** January 08, 2024

**Published:** February 29, 2024

Use your device to scan and read the article online



We aimed to investigate the cardiomyocyte-protective effects of bone marrow mesenchymal stem cells (BMSCs)-derived exosomes on ischemia/reperfusion (I/R)-injured rats and to explore the mechanisms. Cardiomyocytes were divided into control group, ischemia/reperfusion group (I/R group), ischemia/reperfusion+exosome group (I/R+Exo group) or ischemia/reperfusion+exosomes transfected with miR-101a-3p inhibitor group (I/R+Exo inhibitor group). MiR-101a-3p levels were lower in I/R and I/R+Exo inhibitor groups than in control and I/R+Exo groups. Apoptosis rate and cleaved caspase 3 expression were higher in I/R and I/R+Exo inhibitor groups. The levels of superoxide dismutase (SOD) in cardiomyocytes of I/R group and I/R+Exo inhibitor group were lower than those of control group and I/R+Exo group, and the levels of malondialdehyde (MDA) and the relative production of oxygen species clusters (ROS) in cardiomyocytes of I/R group and I/R+Exo inhibitor group were higher than those of control group and I/R+Exo group. The levels of interleukin-10 (IL-10), interleukin-6 (IL-6), tumour necrosis factor  $\alpha$  (TNF- $\alpha$ ), and nuclear factor  $\kappa$ B (NF- $\kappa$ B) were higher in the I/R group and the I/R +Exo inhibitor group than in the control group and the I/R+Exo group. Bioinformatics analysis suggested that Pik3c3 is the most promising gene involved in miR-101a-3p-mediated apoptosis in cardiomyocytes, and in vitro experiments confirmed that low expression of miR-101a-3p significantly up-regulated the mRNA and protein expression levels of Pik3c3. BMSCs-derived exosomes have a protective effect on cardiomyocytes from I/R-injured rats, and the mechanism may be related to the inhibition of oxidative stress and inflammatory responses in cardiomyocytes by exosome-delivered miR-101a-3p.

**Keywords:** Exosomes, Bone marrow mesenchymal stem cells, Cardiomyocytes, Ischemia/reperfusion, miR-101a-3p, Oxidative stress, Inflammatory reaction.

### 1. Introduction

In recent years, cardiovascular diseases (CVDs) have been identified as the leading cause of premature morbidity and mortality in our population. It has been projected that ischaemic heart disease (IHD) has become one of the leading causes of the global burden of disease [1,2]. Currently, there are three main treatments for IHD including pharmacological treatments, percutaneous coronary intervention and coronary artery bypass grafting. The main goal of these treatments is to restore myocardial blood perfusion, however, reperfusion itself can cause additional damage called myocardial ischemia/reperfusion injury (I/R), which reduces even the benefits of myocardial reperfusion. Reperfusion injury ultimately leads to the death of cardiomyocytes that survived before myocardial reperfusion, and this form of myocardial injury itself can induce myocyte death and increase the extent of the infarction, which partly explains why, despite optimal myocardial reperfusion, patients may have a poorer prognosis after an acute myocardial infarction [3].

Myocardial ischemia/reperfusion (I/R) can induce cardiomyocyte apoptosis, myocardial tissue necrosis, and

even cardiac arrest, thus affecting the therapeutic efficacy of cardiac ischemic diseases [4]. Bone marrow mesenchymal stem cells (BMSCs) are an ideal tool for cell therapy and have been applied to I/R treatment. Numerous studies have confirmed that BMSCs can participate in immunomodulation, inflammation suppression, secretion of various cell growth factors and tissue repair, and their cardioprotective effects are mainly achieved by inhibiting apoptosis [5,6]. However, the effectiveness of cell therapy is unstable due to the disadvantages of immune rejection, complicated surgical procedures and low survival rate of transplanted cells.

Exosomes are small membrane vesicles carrying DNA, RNA and proteins, extracellular vesicles with diameters between 40 and 160 nm, usually enriched with various biologically active substances such as proteins, DNA, lncRNAs and miRNAs, which play an important role in exchanging cellular information mainly by transferring genetic material and proteins to target cells [7]. With a deeper understanding of the role of BMSCs in tissue regeneration, more and more studies suggest that this role of BMSCs may be related to their released exosomes [8].

\* Corresponding author.

E-mail address: [13351627345@163.com](mailto:13351627345@163.com) (Q. Li).

Doi: <http://dx.doi.org/10.14715/cmb/2024.70.2.10>

Therefore, BMSCs-derived exosomes may become a new alternative method for the treatment of ischaemic heart disease. Hypoxic preconditioning of stem cells can effectively increase the survival rate of BMSCs after transplantation and enhance their protective effects on damaged tissues, therefore, hypoxic preconditioning may enhance the biological effects of stem cells. In this study, we observed the effects of hypoxic preconditioning of BMSCs-derived exosomes on oxidative stress and myocardial injury in myocardial I/R rats, and explored the effects of hypoxic preconditioning on the function of exosomes in repairing cardiac tissues [9].

MicroRNAs (miRNAs) can mediate gene expression by binding to the 3' translational region (3UTR) of mRNAs. miR-101a-3p has been shown to be widely present in exosomes secreted by BMSCs. miR-101a-3p expression has been reported to be significantly reduced in myocardial tissues of rat myocardium after 4 weeks of myocardial ischemia as compared to normal physiological state [10,11]. This suggests that the expression of miR-101a-3p may play an important role in the process of IR injury, with an inhibitory effect on fibroblast proliferation. However, whether BMSCs-derived exosomes are protective against I/R injury in cardiomyocytes and the role of their delivered miR-101a-3p in this process also needs to be further explored. Therefore, we observed the cardiomyocyte-protective effects of BMSCs-derived exosomes on I/R-injured rats and explored the mechanisms [12].

## 2. Materials and Methods

### 2.1. Rats and reagents

Rat cardiomyocyte H9c2 was obtained from Shanghai cell bank, Chinese Academy of Sciences (Shanghai, China); adult male SD rats, weighing 180-200 g, aged 8-10 weeks. Exo Quick TC exosome extraction kit was purchased from American SBI company; TIANscript RT Kit was purchased from Tiangen Biochemical Technology (Beijing) Co., Ltd. (Beijing, China), Hot Start Fluorescent PCR Core Reagent Kits (SYBR Green I) was purchased from BBI, Italy, rabbit anti-rat hypoxia-inducible factor 1  $\alpha$  (HIF-1 $\alpha$ ) Primary antibodies were purchased from Beijing Zhongshan Jinqiao Biotechnology Co., Ltd. (Beijing, China). Superoxide dismutase (SOD) and malondialdehyde (MDA) kits were purchased from Cayman Company, USA. Interleukin-6 (IL-6), interleukin-10 (IL-10) and tumour necrosis factor- $\alpha$  (TNF- $\alpha$ ) detection kits were purchased from Nanjing Jianjian Bioengineering Research Institute (Nanjing, China), and Bcl-2 and Caspase-3 (Wuhan Beilai Biotechnology Co., Ltd. Wuhan, China).

### 2.2. Cell culture

H9c2 rat cardiomyocytes were cultured in DMEM medium containing 10% fetal bovine serum and 5% penicillin-streptomycin double antibody at 37°C in a 5% CO<sub>2</sub> incubator. When the cell confluence reached more than 85% under the microscope, the first 10 generations of cells with good activity were selected for the experiment by passaging culture according to the ratio of 1:3.

### 2.3. Culture of BMSCs and extraction of exosomes

SD rats were executed by guillotine method, and the femur and tibia were removed after local iodophor disinfection, the bone ends were cut to reveal the bone marrow

cavity. The bone marrow cavity was repeatedly flushed with culture medium, and the obtained flushing solution was centrifuged at 4°C and 2000 g for 5 min in a centrifuge, and the retained precipitate was re-suspended with medium containing 10% fetal bovine serum, and then cultured in adherent wall culture, regular fluid change and passaging culture. The third-generation BMSCs were taken, and flow cytometry was used to characterise the stem cells with a positive rate of more than 99% for the stem cell markers CD29 and CD105, respectively, and exosomes were extracted at the same time.

### 2.4. BMSCs-derived exosomes transfected with miR-101a-3p inhibitor

The 150  $\mu$ L total transfection solution contained 10 L of Exo-Fect solution, 20 pmol miRNA, 70  $\mu$ L of sterile 1 $\times$ PBS, and 50  $\mu$ L of purified exosomes. Exosomes were incubated with the transfection solution at 37°C with shaking for 10 min, and then the reaction was terminated by adding 30  $\mu$ L of Exo Quick-TC reagent to the transfection system in an ice bath for 30 min. The samples were centrifuged at 13000~14000 rpm for 3 min, and then the transfected exosome vesicles were resuspended with 300  $\mu$ L 1 $\times$ PBS for spare parts. miR-101a-3p inhibitor was prepared by Shanghai Gemma Pharmaceutical Technology Co. (Shanghai, China). The sequence was designed as follows: 5'-UUCAGUUAUCACAGUACUGUA-3'.

### 2.5. Grouping, exosome giving and specimen retention methods

After cell suspension concentration was adjusted, cells were inoculated into 96-well plates, cultured overnight, and divided into 4 groups: control group, ischemia-reperfusion group (I/R group), ischemia-reperfusion + exosome group (I/R+Exo group), and ischemia-reperfusion + exosome transfection miR-101a-3p inhibitor group (I/R+Exo inhibitor group). Control group cells were not treated; I/R group cells were first incubated in 3.3 mmol/L H<sub>2</sub>O<sub>2</sub> for 10 minutes and then reoxygenated in DMEM medium for 30 minutes to establish the I/R cell model. I/R+Exo group was established as I/R group, and 2  $\mu$ g/mL exosomes were added to the hypoxia/reperfusion model. I/R+Exo inhibitor group was established as I/R group, and 2  $\mu$ g/mL exosomes were added at the same time. The hypoxia reperfusion model established in the I/R+Exo inhibitor group was the same as that in the I/R group, but 2  $\mu$ g/mL transfected miR-101a-3p inhibitor exosomes were added.

### 2.6. Detection of cell viability

The viability of the cells in each group was detected by MTS method, which was performed according to the instructions of the kit, and the wavelength was set at 490 nm and the absorbance value A<sub>490</sub> was detected in the enzyme lab, and the viability of the cells was calculated according to the formula ((experimental wells A<sub>490</sub> - blank wells A<sub>490</sub>)/(control wells A<sub>490</sub> - blank wells A<sub>490</sub>) $\times$ 100 %).

### 2.7. Detection of apoptosis rate

For the above subgroups, the procedure was as follows: the cells were digested with trypsin without EDTA and washed twice with ice-cold PBS. 400  $\mu$ L of annexin V binding solution was added and left for 15 minutes at 4°C. 5 L of annexin V-FITC was added and stained for 15 min at 4°C. 10  $\mu$ L PI was added and stained for 5 min at 4°C.

Flow cytometry was used for detection.

## 2.8. Determination of cleaved caspase 3 and Bcl-2 expression levels in cardiomyocytes by Western blot

The samples of each group were taken out and transferred to PVDF membrane via 12% SDS-PAGE, and then placed in 5% skimmed milk in a closed shaker at room temperature for 1.5 h. Diluted primary antibodies against cleaved caspase 3, (1:1,000, Bioss, Woburn, MA, USA), and Bcl-2 (1:1,000, Bioss, Woburn, MA, USA) were added respectively, and the samples were incubated overnight at 4°C. The samples were incubated at 4°C for 1.5 h. After washing the membrane with Tris-HCl buffer salt solution (TBST) and shaking, the membrane was incubated with secondary antibody for 1 h. The membrane was washed with TBST three times, and the ODYSSEY imaging system was used to scan the SLC7A11 and GPX4 bands with GADPH (1:1000, Abcam, Cambridge, MA, USA) as the reference protein, and analyze the grey values of the bands with Image J software.

## 2.9. Determination of SOD, MDA and ROS content in each group

According to the SOD and MDA kit instructions, the absorbance values at specific wavelengths were obtained using a spectrophotometer, and the expression levels of SOD and MDA were calculated from the absorbance values and the standard curve. For the detection of reactive oxygen cluster (ROS) generation in each group, DHE reaction solution was added dropwise and protected from light according to the DHE assay kit instructions, and the slices were washed in PBS solution and placed under a laser confocal microscope for observation and image acquisition, and the fluorescence intensity of the slices was analysed using Image J software. The relative DHE fluorescence intensity ratio was used to express the relative ROS production of rat cardiomyocytes in each group.

## 2.10. Observation of inflammatory reaction of rats in each group

According to the kit instructions of IL-10, IL-6 and TNF- $\alpha$ , use a spectrophotometer to obtain the absorbance value at a specific wavelength, and calculate expression levels of iNOS, IL-6 and TNF- $\alpha$  through the absorbance value and standard curve. NF- $\kappa$ B was detected by immunofluorescence staining.

## 2.11. Statistical analysis

Statistic Package for Social Science (SPSS) 25.0 software (IBM, Armonk, NY, USA) was used for statistical processing. The experimental data were all metrological data, expressed as mean  $\pm$  standard deviation. One-way analysis of variance was used for comparison among multiple groups, and LSD-*t* test was further used for the data with statistical differences.  $P < 0.05$  was statistically significant.

## 3. Results

### 3.1. Identification and uptake of exosomes

According to the extraction method described above, exosomes were obtained, and the exosomes were observed under transmission electron microscopy as round, membranous vesicles with a double membrane structure (Figure 1A). The above results indicated that the material extrac-

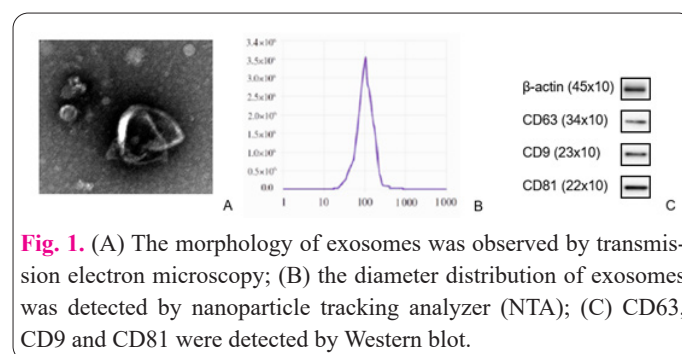
ted by ultracentrifugation was identified as exosomes. The results of particle size analysis of exosomes by particle size analyser showed linear and smooth MODE curves, and the size of exosome diameters was more concentrated, as reported in the classical literature between 3-150 nm, with the mean of the peak particle size of 112 nm, respectively (Figure 1B). The results of Western blot showed that the exosomes expressed the surface marker proteins of the exosomes: CD63, CD9 and CD81 (Figure 1C).

### 3.2. Comparison of relative expression of miR-101a-3p in cardiomyocytes of rats in each group

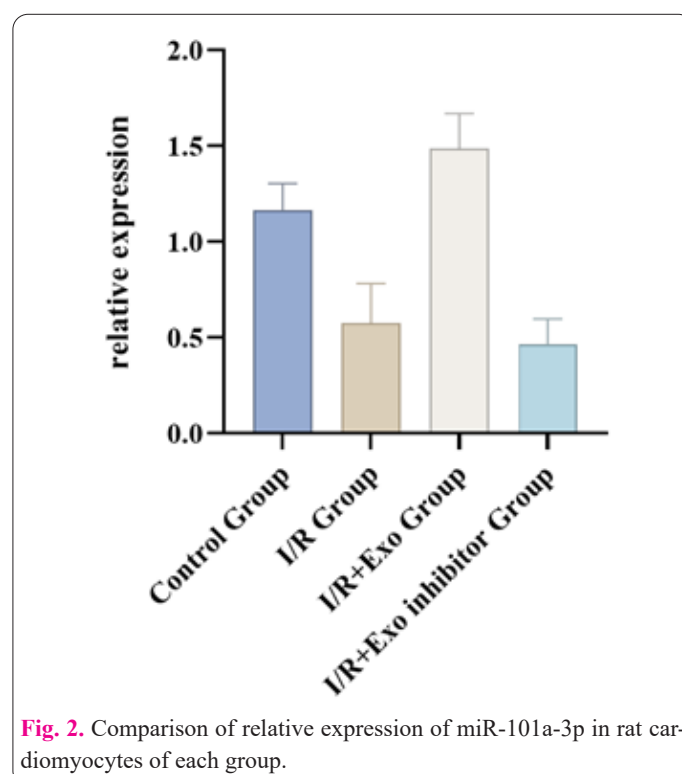
The relative expression of miR-101a-3p in cardiomyocytes of rats in the control group, I/R group, I/R+Exo group, and I/R+Exo inhibitor group were  $1.17 \pm 0.14$ ,  $0.57 \pm 0.21$ ,  $1.49 \pm 0.18$ , and  $0.46 \pm 0.13$ , respectively. The relative expression of miR-145-5p in cardiomyocytes of rats in the I/R group and I/R+Exo inhibitor group were lower than those in the control group and I/R+Exo group ( $P < 0.05$ ), and the relative expression of miR-101a-3p in cardiomyocytes of rats in the control group was lower than that in I/R+Exo inhibitor group ( $P < 0.05$ ), see Figure 2.

### 3.3. Comparison of cardiomyocyte apoptosis rate and relative expression of apoptosis protein cleaved caspase 3 and Bcl-2 in each group

See Table 1 and Figure 3 for the comparison of cardio-



**Fig. 1.** (A) The morphology of exosomes was observed by transmission electron microscopy; (B) the diameter distribution of exosomes was detected by nanoparticle tracking analyzer (NTA); (C) CD63, CD9 and CD81 were detected by Western blot.

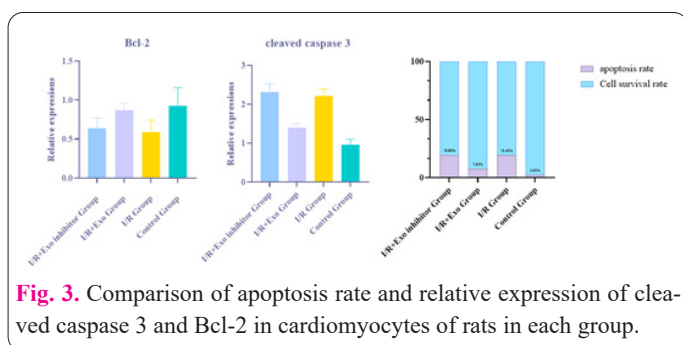


**Fig. 2.** Comparison of relative expression of miR-101a-3p in rat cardiomyocytes of each group.

**Table 1.** Comparison of cardiomyocyte apoptosis rate and relative expression of apoptotic proteins cleaved caspase 3 and Bcl-2 in each group ( $\bar{x}\pm s$ ).

Group	Apoptosis rate	Relative expression	
		cleaved caspase 3	Bcl-2
I/R+Exo inhibitor group	19.76%*#	2.31±0.21*#	0.63±0.13*#
I/R+Exo group	7.85%*	1.39±0.11*	0.87±0.09
I/R group	19.12%*#	2.21±0.19*#	0.59±0.16*#
Control group	2.60%	0.96±0.14	0.92±0.24

Note: compared with the control group, \* $P<0.05$ ; compared with I/R+Exo group, # $P<0.05$ .

**Fig. 3.** Comparison of apoptosis rate and relative expression of cleaved caspase 3 and Bcl-2 in cardiomyocytes of rats in each group.

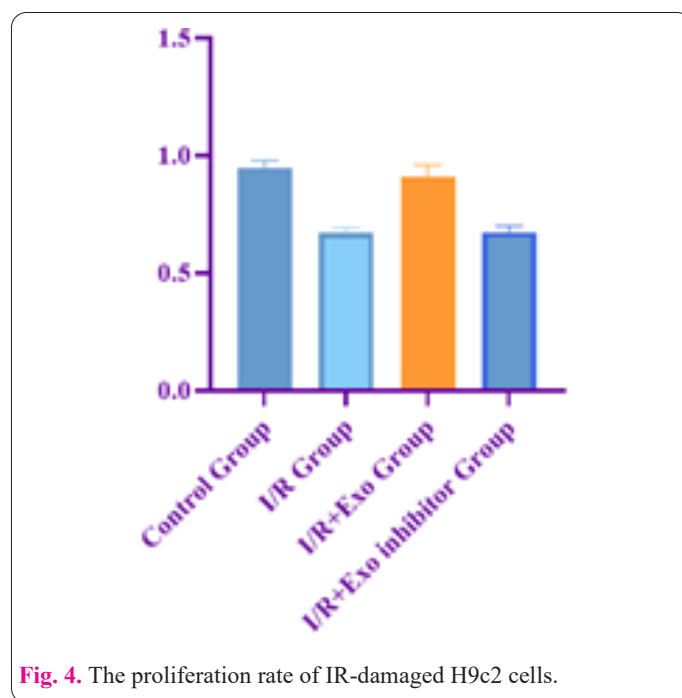
myocyte apoptosis rate and relative expression of apoptotic proteins cleaved caspase 3 and Bcl-2 in each group. According to Table 1, the apoptosis rate of cardiomyocytes and the relative expression of cleaved caspase 3 in the I/R group and I/R+Exo inhibitor group were higher than those in the control group and I/R+Exo group ( $P<0.05$ ). Compared with the control group, the bcl-2 protein expression level in the I/R group was significantly reduced ( $P<0.05$ ), and the apoptosis rate of cardiomyocytes and the relative expression of cleaved caspase 3 and Bcl-2 in the I/R+Exo group were higher than those in the control group ( $P<0.05$ ).

### 3.4. Effect of miR-101a-3p on proliferation ability of IR-damaged H9c2 cells

Compared with the control group, the cell proliferation ability of I/R group and I/R+Exo inhibitor group was significantly reduced ( $P<0.01$ ); compared with the I/R group and I/R+Exo inhibitor group, the cell proliferation ability of I/R+Exo group was significantly elevated ( $P<0.01$ ), but there was no significant difference ( $P>0.05$ ) compared with the control group, as shown in Figure 4.

### 3.5. Comparison of oxidative stress levels in rat cardiomyocytes in each group

Comparison of SOD, MDA levels and relative ROS production in rat cardiomyocytes of each group is shown in Table 2 and Figure 5. As can be seen from Table 2, SOD levels in I/R group and I/R + Exo inhibitor group were

**Fig. 4.** The proliferation rate of IR-damaged H9c2 cells.

lower than those in control group and I/R + Exo group (both  $P<0.05$ ), and MDA levels and relative ROS production in I/R group and I/R + Exo inhibitor group were higher than those in Sham group and I/R + Exo group ( $P<0.05$ ).

### 3.6. Comparison of IL-10, IL-6, TNF- $\alpha$ and NF- $\kappa$ B levels in rat cardiomyocytes of different groups

A comparison of the levels of IL-10, IL-6, TNF- $\alpha$ , and NF- $\kappa$ B in rat cardiomyocytes of each group is shown in Table 3, which shows that the levels of IL-10, IL-6, TNF- $\alpha$ , and NF- $\kappa$ B in rat cardiomyocytes of the I/R group and the I/R+Exo inhibitor group were higher than those of the Sham group and the I/R+Exo group ( $P<0.05$ ) (Table 3, Figure 6).

### 3.7. Potentially regulated mRNAs by miR-101a-3p

To investigate the molecular mechanisms by which miR-101a-3p regulates cardiomyocyte death-regulating

**Table 2.** Comparison of SOD and MDA levels and relative ROS production in each group ( $\bar{x}\pm s$ ).

Group	SOD(U/g)	MDA( $\mu$ mol/g)	ROS
I/R+Exo inhibitor group	13.72±1.67*#	10.11±0.74*#	2.23±0.14*#
I/R+Exo inhibitor group	18.36±2.02	4.81±0.36	1.34±0.21
I/R group	13.86±1.82*#	10.34±0.67*#	2.27±0.17*#
Sham group	19.75±2.11	4.62±0.61	1.29±0.19

Note: Comparison with control group, \* $P<0.05$ ; comparison with I/R + Exo group, # $P<0.05$ .

**Table 3.** Comparison of IL-10, IL-6, TNF- $\alpha$ , and NF- $\kappa$ B levels in rat cardiomyocytes in each group ( $\bar{x}\pm s$ ).

Group	NF- $\kappa$ B	IL-10(ng/L)	IL-6(ng/L)	TNF- $\alpha$ (ng/L)
I/R+Exo inhibitor group	2.60 $\pm$ 0.13**	35.82 $\pm$ 4.82**	413.21 $\pm$ 39.67**	49.76 $\pm$ 3.26**
I/R+Exo inhibitor group	1.25 $\pm$ 0.12	30.74 $\pm$ 3.11	230.27 $\pm$ 34.15	31.91 $\pm$ 3.32
I/R group	2.61 $\pm$ 0.12**	35.70 $\pm$ 4.54**	415.15 $\pm$ 31.73**	53.27 $\pm$ 3.41**
Sham group	1.04 $\pm$ 0.14	29.08 $\pm$ 2.57	212.89 $\pm$ 24.52	29.36 $\pm$ 4.91

Note: Compared with Sham group, \* $P$ <0.05; compared with I/R+Exo group, # $P$ <0.05.

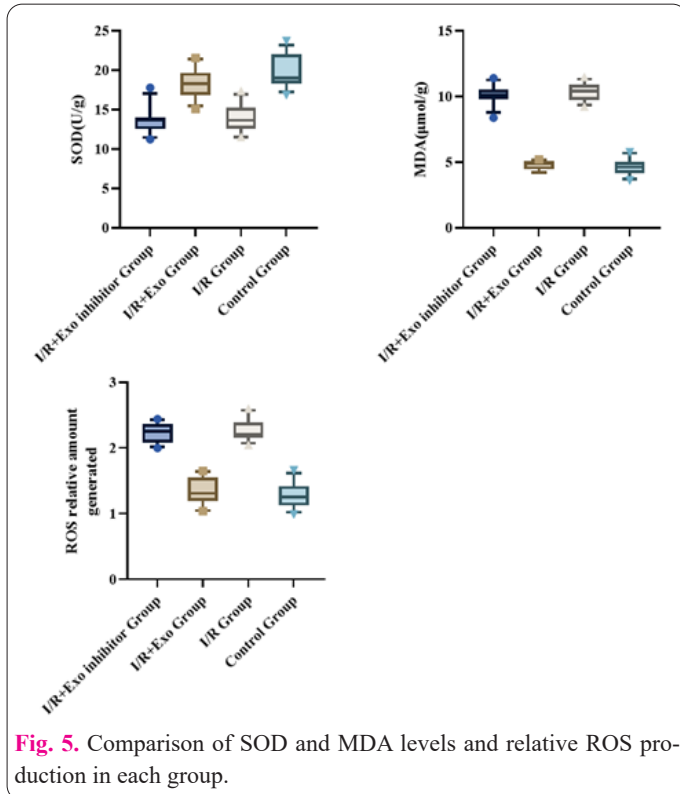


**Fig. 5.** Comparison of SOD and MDA levels and relative ROS production in each group.

functions, the intersection of predicted targets of miR-101a-3p using TargetScan, starBase, and miRDB databases revealed 93 genes that could be target genes of miR-101a-3p. Kyoto Encyclopedia of Genes and Genomes (KEGG) enrichment analysis showed that the oncogene (rat sarcoma virus, Ras) signaling pathway PI3K-Akt signaling pathway and others may be involved in the regulation of the above process (Figure 7). GeneOntology (GO) enrichment analysis showed that 256 target genes were involved in biological processes such as cell cycle, mRNA processing and protein binding regulation (Figure 8).

### 3.8. Pik3c3 is a direct target of miR-101a-3p in cardiomyocytes

Bioinformatics analysis results suggested that Pik3c3 is the most promising gene involved in miR-101a-3p-mediated apoptosis in cardiomyocytes. In vitro experiments confirmed that low expression of miR-101a-3p significantly upregulated the mRNA and protein expression levels of /Pik3c3 ( $P$ <0.01, Figure 9).

## 4. Discussion

I/R injury can affect the functions of many organs and tissues, including brain, heart, liver, lung, kidney, skeletal muscle, testicular tissue and endothelial tissue. The heart is a highly perfused organ, which is more sensitive to ischemia and hypoxia [13,14]. Acute heart injury caused by I/R is a complex pathological process with multiple factors and pathways, which can cause prolonged hospitaliza-

tion time, increased complications and mortality based on the primary disease. Over the years, people have worked hard to find appropriate methods to prevent and treat the disease. Current studies have found that cardiac I/R injury involves a variety of pathological mechanisms, in which oxidative stress injury and inflammatory response play important roles. In the ischemic heart and subsequent reoxygenation process, the production of ROS in the reperfusion phase initiates a series of harmful cellular responses, leading to inflammation, cell death and acute heart failure. In the process of I/R, the damaged tissues produce excessive ROS to cause oxidative stress and change mitochondrial oxidative phosphorylation, leading to ATP depletion, intracellular calcium increase and activation of membrane

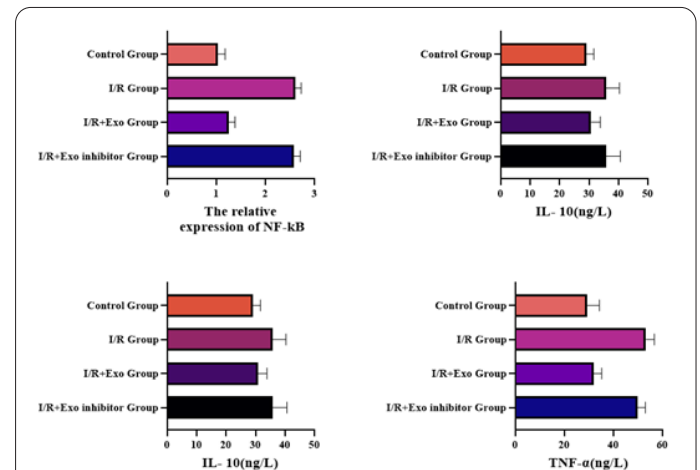


**Fig. 6.** Comparison of IL-10, IL-6, TNF- $\alpha$ , and NF- $\kappa$ B levels in rat cardiomyocytes in each group.

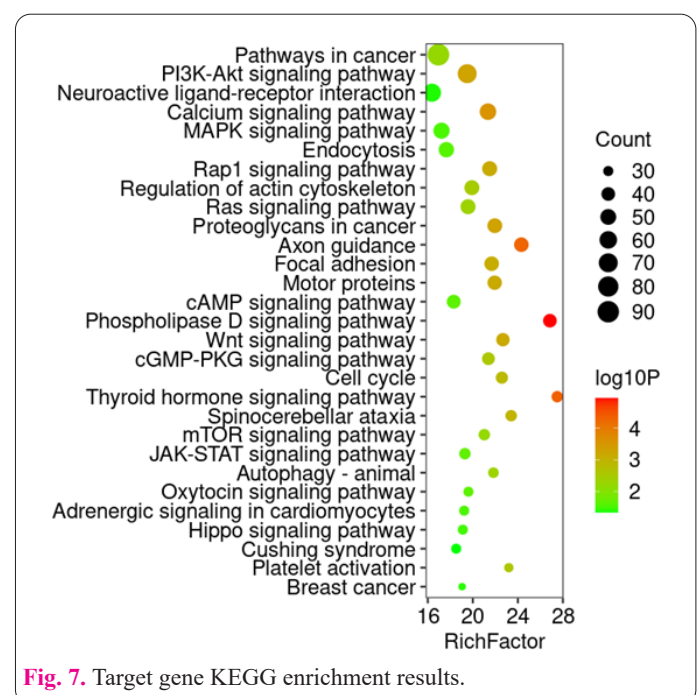


**Fig. 7.** Target gene KEGG enrichment results.

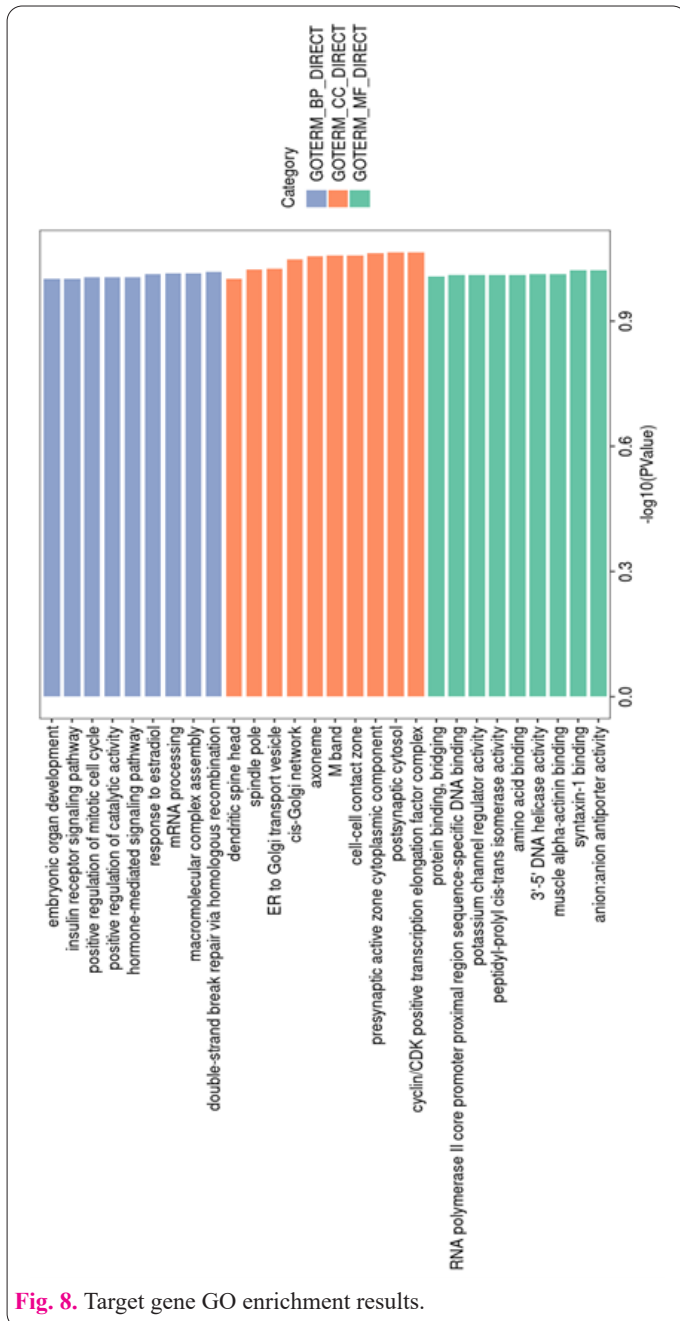
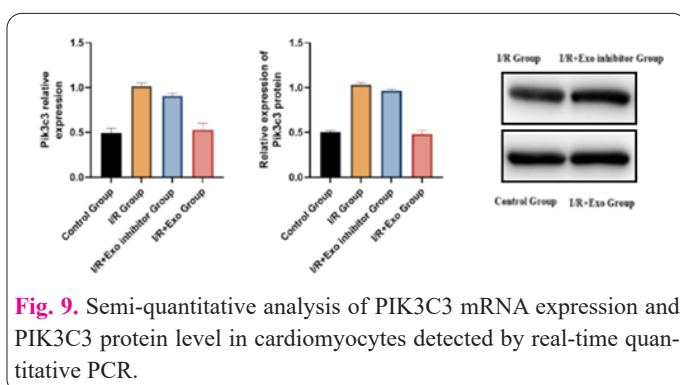


**Fig. 8.** Target gene GO enrichment results.



phospholipid proteases [15,16]. Oxygen free radicals can be produced in the blood flow during I/R reperfusion period, leading to lipid peroxidation, which is the main way of free radical damage to tissues. The formation of free radicals promotes apoptosis and cell death through membrane lipid peroxidation and oxidative damage of proteins and DNA to develop cardiomyocyte damage. Therefore, inhibiting this pathway or preventing free radical produc-

tion is an important strategy to protect cardiomyocytes during I/R. Proinflammatory cells such as IL-1 $\alpha$ , IL-6 and TNF- $\alpha$  It is the main mediator of inflammatory response and regulates the expression of adhesion molecules, leukocyte infiltration and activation.

The decrease of adenosine triphosphate (ATP) produced by mitochondria in ischemic cardiomyocytes during the occurrence of I/R led to the accumulation of Ca<sup>2+</sup> in mitochondria, which damaged the basic mitochondrial function, thus causing the dysfunction of cellular respiratory chain; at the same time, due to the decrease of SOD production in cardiomyocytes, it led to the increase of the accumulation of oxygen radicals generation, which eventually led to the continuous generation of ROS [17]. The results of this study showed that the SOD levels in both the I/R group and the I/R+Exo inhibitor group were lower than those in the control group and the I/R+Exo group (both  $P < 0.05$ ), and the MDA levels and relative ROS generation in both the I/R group and the I/R+Exo inhibitor group were higher than those in the Sham group and the I/R+Exo group (both  $P < 0.05$ ); this suggests that BMSCs-derived exosomes could better inhibit the oxidative stress response caused by I/R. HIF-1 $\alpha$  is considered to be a major transcription factor regulating tissue cell response to hypoxia during ischemic events. At the onset of I/R, hypoxic conditions induce HIF-1 $\alpha$  activation, which in turn improves oxygen supply to tissues in the ischemic region by increasing angiogenic proteins, inhibiting mitochondrial function, and switching metabolism from oxidative to glycolytic pathways. Studies have confirmed the inhibitory effect of HIF-1 $\alpha$  on myocardial I/R injury. The results of the present study showed that the levels of IL-10, IL-6, TNF- $\alpha$ , and NF- $\kappa$ B in rat cardiomyocytes in the I/R group and the I/R+Exoinhibitor group were higher than those in the Sham group and the I/R+Exo group (both  $P < 0.05$ ); this suggests that the mechanism related to the attenuation of cardiac muscle injury caused by I/R by exosomes derived from BMSCs may be related to their elevated HIF-1 $\alpha$  expression. In conclusion, the mechanism by which BMSCs-derived exosomes attenuated myocardial injury in I/R rats and enhanced their protective effects on myocardium may be related to the induction of up-regulation of HIF-1 $\alpha$  expression in BMSCs-derived exosomes and attenuation of myocardial tissue oxidative stress.

Currently, researchers focus the study of exosome action mechanisms on anti-apoptosis, anti-inflammation, promotion of angiogenesis, antioxidants, anti-fibrosis and so on. Exosomes regulate the biological behavior of cells and tissues in the body by carrying or delivering bioinformatic substances such as proteins and RNAs to play the above roles and achieve the effect of improving myocardial cell injury. Among them, the key role of RNAs carried by exosomes in it has received more and more attention. It has also been found that miRNA deletion significantly decreased the repair ability of MSCs and their exosomes to cardiomyocyte injury, suggesting that miRNAs play a key role in the repair process. The above studies suggest that miRNAs transferred by exosomes are biologically active and can target regulate the levels of mRNAs in the cells after entering the target cells and thus play a role [18]. The above studies suggest that miRNAs transferred by exosomes are biologically active and can target regulate the levels of mRNAs in the cells after entering the target cells and thus play a role. miR-101a-3p has been shown to be a

tumor suppressor, which can inhibit tumor cell proliferation, migration, and invasion in a variety of tumors such as esophageal cancer cells, bladder cancer, colon cancer, etc. miR-101a-3p expression was reduced in a lipopolysaccharide-induced acute lung injury model, in which overexpression of miR-101a-3p inhibited IL-1 $\beta$ , IL-6, and TNF- $\alpha$  expression and NF- $\kappa$ B and ROS activation, thereby exerting a protective effect. No miR-101a-3p-related studies have been reported in the field of cardiac I/R injury.

miRNAs are key players in post-transcriptional regulation. Currently, miR-101a-3p has been shown to regulate its gene targets and participate in the regulation of biological processes such as cell proliferation and apoptosis [19]. For example, miR-101a-3p can regulate myoblast proliferation and differentiation by targeting transforming growth factor B receptor 1. However, the mechanism of miR-101a-3p targeting regulation in IR injury has been less studied. In the present study, we found that miR-101a-3p, whose direct target is *Pik3c3*, can activate the *Pik3-Akt* pathway and thus significantly inhibit pathological autophagy in cardiomyocytes, thereby attenuating cellular oxidative stress and apoptosis. In the present study, we clarified that *Pik3c3* is a target gene of miR-101a-3p, which is involved in miR-101a-3p-mediated cardiomyocyte apoptosis. Our results suggest that miR-101a-3p promotes cardiomyocyte apoptosis by negatively regulating *Pik3c3* [20].

AKT activation can regulate multiple downstream target proteins, such as regulation of apoptosis, survival, and phosphorylation of mTOR proteins. mTOR, an atypical serine/threonine protein kinase, acts as a downstream effector protein of AKT, regulates transcription and protein synthesis, and has an important impact on cell growth and apoptosis. It has been shown that serum exosomal miR-101a-3p promotes cardiac fibroblast proliferation by regulating the AKT/mTOR signaling pathway in cardiac fibroblasts [21]. Taken together, these findings support a pro-apoptotic role of miR-101a-3p in cardiomyocytes at least in part through inhibition of *Pik3c3* expression and phosphorylation of AKT/mTOR. In summary, VM-Exos promotes VM development by affecting apoptosis in cardiomyocytes. miR-101a-3p enriched in exosomes is derived from cardiomyocytes and plays an important role in cardiomyocyte apoptosis by targeting *Pik3c3* and inhibiting the AKT/mTOR pathway. These findings suggest that the use of nanomaterials in combination with miR-101a-3p inhibitors may be a promising therapeutic approach to alleviate I/R progression.

### Conflict of interests

The author has no conflicts with any step of the article preparation.

### Consent for publications

The author read and approved the final manuscript for publication.

### Ethics approval and consent to participate

This study was approved by the Animal Ethics Committee of The Third Affiliated Hospital of Qiqihar Medical University Animal Center.

### Informed consent

The authors declare not used any patients in this research.

### Availability of data and material

The data that support the findings of this study are available from the corresponding author upon reasonable request.

### Authors' contributions

Di Zhao and Qiang Li designed the study and performed the experiments, Yanling Bu and Haifeng Shao collected the data, Jian Wang and Wenhua Li analyzed the data, Di Zhao and Qiang Li prepared the manuscript. All authors read and approved the final manuscript.

### Funding

This work was supported by The Basic Scientific Research Fund Research Project of Heilongjiang Provincial University in 2022, the project name is "The Protective Effect of Exosomes Derived from Bone Marrow Mesenchymal Stem Cells on Cardiomyocyte Hypoxia Reperfusion Injury" (project number: 2022-KYYWF-0813).

### References

- Severino P, D'Amato A, Pucci M, Infusino F, Adamo F, Birtolo LI et al (2020) Ischemic Heart Disease Pathophysiology Paradigms Overview: From Plaque Activation to Microvascular Dysfunction. *Int J Mol Sci* 21:8118. doi: 10.3390/ijms21218118
- Cai W, Xu D, Zeng C, Liao F, Li R, Lin Y et al (2022) Modulating Lysine Crotonylation in Cardiomyocytes Improves Myocardial Outcomes. *Circ Res* 131:456-472. doi: 10.1161/CIRCRESAHA.122.321054
- Ma Y, Su M, Qian W, Xuan Y, Chen T, Zhou R et al (2023) CXCR4-overexpressed exosomes from cardiosphere-derived cells attenuate myocardial ischemia/reperfusion injury by transferring miRNA to macrophages and regulating macrophage polarization. *Cell Mol Biol* 69:98-103. doi: 10.14715/cmb/2023.69.12.16
- Chen C, Chen Y, Xu M, Chen L, Sun Z, Gong J et al (2023) Curcubitacin B protects against myocardial ischemia-reperfusion injury through activating JAK2/STAT3 signaling pathway. *Cell Mol Biol* 69:155-161. doi: 10.14715/cmb/2023.69.11.23
- El AE, Kramann R, Schneider RK, Li X, Seeger W, Humphreys BD et al (2017) Mesenchymal Stem Cells in Fibrotic Disease. *Cell Stem Cell* 21:166-177. doi: 10.1016/j.stem.2017.07.011
- Xu R, Zhang F, Chai R, Zhou W, Hu M, Liu B et al (2019) Exosomes derived from pro-inflammatory bone marrow-derived mesenchymal stem cells reduce inflammation and myocardial injury via mediating macrophage polarization. *J Cell Mol Med* 23:7617-7631. doi: 10.1111/jcmm.14635
- He L, He T, Xing J, Zhou Q, Fan L, Liu C et al (2020) Bone marrow mesenchymal stem cell-derived exosomes protect cartilage damage and relieve knee osteoarthritis pain in a rat model of osteoarthritis. *Stem Cell Res Ther* 11:276. doi: 10.1186/s13287-020-01781-w
- Liu S, Fan M, Xu JX, Yang LJ, Qi CC, Xia QR et al (2022) Exosomes derived from bone-marrow mesenchymal stem cells alleviate cognitive decline in AD-like mice by improving BDNF-related neuropathology. *J Neuroinflamm* 19:35. doi: 10.1186/s12974-022-02393-2
- Zhu B, Zhang L, Liang C, Liu B, Pan X, Wang Y et al (2019) Stem Cell-Derived Exosomes Prevent Aging-Induced Cardiac Dysfunction through a Novel Exosome/lncRNA MALAT1/NF-kappaB/TNF-alpha Signaling Pathway. *Oxid Med Cell Longev* 2019:9739258. doi: 10.1155/2019/9739258
- Huang C, Luo W, Wang Q, Ye Y, Fan J, Lin L et al (2021) Human mesenchymal stem cells promote ischemic repairment and angiogenesis of diabetic foot through exosome miRNA-21-5p. *Stem*

- Cell Res 52:102235. doi: 10.1016/j.scr.2021.102235
11. Wang J, Lee CJ, Deci MB, Jasiewicz N, Verma A, Canty JM et al (2020) MiR-101a loaded extracellular nanovesicles as bioactive carriers for cardiac repair. *Nanomedicine-Uk* 27:102201. doi: 10.1016/j.nano.2020.102201
  12. Zhai C, Hu H, Tang G, Pan H, Zhang Y, Qian G (2020) MicroRNA-101a protects against the H<sub>2</sub>O<sub>2</sub>-induced injury on cardiomyocytes via targeting BCL2L1. *Am J Transl Res* 12:2760-2768.
  13. Zhou M, Yu Y, Luo X, Wang J, Lan X, Liu P et al (2021) Myocardial Ischemia-Reperfusion Injury: Therapeutics from a Mitochondria-Centric Perspective. *Cardiology* 146:781-792. doi: 10.1159/000518879
  14. Zhao WK, Zhou Y, Xu TT, Wu Q (2021) Ferroptosis: Opportunities and Challenges in Myocardial Ischemia-Reperfusion Injury. *Oxid Med Cell Longev* 2021:9929687. doi: 10.1155/2021/9929687
  15. Bugger H, Pfeil K (2020) Mitochondrial ROS in myocardial ischemia reperfusion and remodeling. *Bba-Mol Basis Dis* 1866:165768. doi: 10.1016/j.bbadis.2020.165768
  16. Li W, Li W, Leng Y, Xiong Y, Xia Z (2020) Ferroptosis Is Involved in Diabetes Myocardial Ischemia/Reperfusion Injury Through Endoplasmic Reticulum Stress. *Dna Cell Biol* 39:210-225. doi: 10.1089/dna.2019.5097
  17. Kalogeris T, Baines CP, Krenz M, Korthuis RJ (2016) Ischemia/Reperfusion. *Compr Physiol* 7:113-170. doi: 10.1002/cphy.c160006
  18. Keshtkar S, Azarpira N, Ghahremani MH (2018) Mesenchymal stem cell-derived extracellular vesicles: novel frontiers in regenerative medicine. *Stem Cell Res Ther* 9:63. doi: 10.1186/s13287-018-0791-7
  19. Zou Y, Li L, Li Y, Chen S, Xie X, Jin X et al (2021) Restoring Cardiac Functions after Myocardial Infarction-Ischemia/Reperfusion via an Exosome Anchoring Conductive Hydrogel. *Acs Appl Mater Inter* 13:56892-56908. doi: 10.1021/acsami.1c16481
  20. Lin B, Xu J, Wang F, Wang J, Zhao H, Feng D (2020) LncRNA XIST promotes myocardial infarction by regulating FOS through targeting miR-101a-3p. *Aging (Albany Ny)* 12:7232-7247. doi: 10.18632/aging.103072
  21. Lee SM, Choi H, Yang G, Park KC, Jeong S, Hong S (2014) microRNAs mediate oleic acid-induced acute lung injury in rats using an alternative injury mechanism. *Mol Med Rep* 10:292-300. doi: 10.3892/mmr.2014.2155